Theory of magnetoresistance anisotropy in the lamellar underdoped copper oxides

E. V. Gomonaj and V. M. Loktev
National Technical University of Ukraine "KPI," 37, ave Peremogy, 03056, Kyiv, Ukraine
(Received 22 November 2000; published 18 July 2001)

The phenomenologic theory of anisotropic magnetoresistance in the underdoped easy-plane antiferromagnets of $YBa_2Cu_3O_x$-type is developed. The observed field-induced anisotropy of the magnetoresistance is explained by the macroscopic symmetry of the sample that for low-field value arises from the redistribution of magnetoelastic antiferromagnetic domains. The field and angular dependencies of the resistivity tensor are in satisfactory agreement with the available experimental data for the low-field (polydomain) and high-field (single-domain) regions.

DOI: 10.1103/PhysRevB.64.064406 PACS number(s): 75.50.Ee, 75.60.Ch, 74.72.Bk

I. INTRODUCTION

The measurements[1–3] of the magnetoresistance (MR) of the heavily underdoped cuprates $R\mathrm{Ba_2Cu_3O}_x$ (R is the rare-earth element), which still preserve an easy-plane antiferromagnetic (AFM) order, show that (1) the electric resistivity of the crystals has a metallic character at high temperatures and grows slower than expected for the hopping electron transport at low T;[4,5] (2) the magnetic field $\mathbf{H}$ applied in the ab plane induces the anisotropy of the magnetoresistance (AMR); (3) the AMR is proportional to $\mathbf{H}^2$ and saturates depending on temperature at $H \leqslant 3-5$ T; (4) the field-induced part of the resistance switches in sign with turning of $\mathbf{H}$ from in parallel to perpendicular toward the current direction; (5) the AMR and its saturation field decrease gradually while approaching the Néel point; (6) after the field is removed, the resistance isotropy is mainly restored, although some residual anisotropy is observed at low temperature.

The $R\mathrm{Ba_2Cu_3O}_x$ cuprates of low ($x<6.4$) oxygen content have near tetragonal crystal structure with the vanishingly small orthorhombic distortions in the paramagnetic phase. The Néel temperature varies from sample to sample, e.g., $T_N=195$ K for $R=\mathrm{Tm}$, $x=6.3$ (Ref. 1) and $T_N=250$ K for $R=\mathrm{Y}$, $x=6.35$.[6] The AFM structure is the collinear one with the cooper spins being aligned in [100] or [010] ab plane directions. Neutron diffraction[6] and ESR (Refs. 3 and 7) on a $YBa_2Cu_3O_x$ single crystal point to the presence of the two types of AFM domains with an orthogonal orientation of the magnetic vectors. So, it seems quite reasonable to assume, as was done in Refs. 1 and 3, that it is the AFM domain structure (DS) that could govern the field and temperature dependence of AMR in the above-mentioned layered compounds.[8]

The present paper is aimed at the development of the simple model of the AMR based on rearrangement of AFM DS under the influence of the external magnetic field.

II. FIELD DEPENDENCE OF RESISTIVITY

The starting point in a phenomenological description of the MR in the magnetically ordered crystals is the separation of the contribution of the magnetic structure into the resisitivity tensor $\hat{\rho}(\mathbf{H})$. In view of the small value of the MR in $R\mathrm{Ba_2Cu_3O}_x$ crystals [less than 0.5% (Refs. 1 and 2)], the formal expression may be obtained by expansion in powers of the structural magnetic vectors with due account of the crystal symmetry. The field dependence of the resisitivity then steams from the modification of the magnetic structure under the action of the external field $\mathbf{H}$.

The magnetic structure of $R\mathrm{Ba_2Cu_3O}_x$ consists of a stacking along the c direction of the weakly coupled pairs of the AFM-ordered copper planes.[6] The interplanar exchange, which is essentially less than the intraplanar one, favors also the AFM ordering of the nearest planes. Under the action of the external magnetic field the magnetic moments in different planes rotate identically, so, in this case the magnetic structure of the crystal may be effectively described by a two-sublattice model[10] with the magnetizations $\mathbf{M}_1$ and $\mathbf{M}_2$. Of more convenience is the AFM $\mathbf{L}=\mathbf{M}_1-\mathbf{M}_2$ vector, which describes the magnetic order, and the FM $\mathbf{M}=\mathbf{M}_1+\mathbf{M}_2$ vector, which is thermodynamically conjugated to the external field.

Thus, the resistivity tensor can be represented as

$$\begin{aligned}
\rho_{XX}(\mathbf{H}) &= \rho_{aa}^{(0)} + \eta_{11}^{L} L_X^2 + \eta_{12}^{L} L_Y^2 + \eta_{111}^{L} L_X^4 + \eta_{112}^{L} L_X^2 L_Y^2 \\
&\quad + \eta_{122}^{L} L_Y^4 + \cdots, \\
\rho_{YY}(\mathbf{H}) &= \rho_{bb}^{(0)} + \eta_{12}^{L} L_X^2 + \eta_{11}^{L} L_Y^2 + \eta_{122}^{L} L_X^4 + \eta_{112}^{L} L_X^2 L_Y^2 \\
&\quad + \eta_{111}^{L} L_Y^4 + \cdots, \\
\rho_{ZZ}(\mathbf{H}) &= \rho_{cc}^{(0)} + \eta_{31}^{L} (L_X^2 + L_Y^2) + \eta_{312}^{L} L_X^2 L_Y^2 + \cdots, \\
\rho_{XY}(\mathbf{H}) &= \eta_{66}^{L} L_X L_Y + \cdots,
\end{aligned} \tag{1}$$

where the coordinate axes X, Y, and Z are directed along $[100]||\mathbf{a}$, $[010]||\mathbf{b}$, and $[001]||\mathbf{c}$, correspondingly and we have substituted the ellipses instead of the terms immaterial for further consideration. In the paramagnetic phase that corresponds to the D_{4h} point group, the resistivity tensor is characterized by only two different components $\rho_{aa}^{(0)}=\rho_{bb}^{(0)} \neq \rho_{cc}^{(0)}$. The 4- and 6-rank tensors $\hat{\eta}^L$ written in the contracted Voigt notations are the macroscopic (phenomenologic) coefficients also invariant with respect to the D_{4h} point group. They account for the transport properties of the substance including the cross sections of the electron-magnon scattering.

In the case of the polydomain crystal, Eqs. (1) should be averaged over the sample volume. So, to study the field dependence of AMR, one should account for the distribution of AFM vectors in the sample.

III. ''STRAY'' ENERGY

Because of the spin-lattice coupling, two types of the orientational AFM domains are characterized by the different spontaneous strain tensors and thus can be treated as magnetoelastic. Due to the rhombic strains, each AFM domain has different physical properties along and perpendicular to the **L** direction. Formation of the thermodynamically equilibrium DS can be governed by the two mechanisms both resulting in creation of zero averaged strains in the field-free sample. The first one is the surface tension on the sample surface or interface of the smallest element of sample microstructure with the special orientation (the surface normal being directed along the principal axis of the crystal).[12] The second and maybe more essential mechanism is due to the finite-size effect and volume-proportional contribution into the free energy from the sample shape.[13] These mechanisms result from the long-range character of the elastic forces and magnetoelastic effects, but the first one can be neglected at low temperatures when the surface relaxation time is much less than the time of observation. Nevertheless, both mechanisms give rise to the effect analogous to demagnetization in FM and can be described by introducing the shape-dependent ''stray'' energy F_{stray}. The main contribution into ''stray'' energy, as it was shown in Ref. 13, arises from the strain tensor $\hat{u}$, averaged over the crystal volume V: $\langle\hat{u}\rangle=(1/V)\int_V d\mathbf{r}\hat{u}$. For the thin [001]-oriented sample the density of the ''stray'' energy may be written as

$$F_{stray}=\frac{1}{2}\alpha'\langle u_{XX}-u_{YY}\rangle^2+2\alpha_{66}\langle u_{XY}\rangle^2. \tag{2}$$

The coefficients α include a contribution from the term proportional to the corresponding elastic modulus of the crystal and from the surface tension[14] as well.

The equilibrium inhomogeneous magnetic (domain) structure arises from the competition of the ''stray'' energy that tends to conserve the shape of the sample through the setting of all the averaged strains and AFM vectors to zero, and the local energy,

$$F_{loc}=\sum_j \xi_j\Big\{-\beta_\perp^{(4)}M_0^2\cos 4\varphi^{(j)}-\frac{\mathbf{H}^2}{2J}\sin^2(\varphi^{(j)}-\psi) + (1/2)c'(u_{XX}^{(j)}-u_{YY}^{(j)})^2+2c_{66}(u_{XY}^{(j)})^2+4M_0^2\lambda_1(u_{XX}^{(j)} - u_{YY}^{(j)})\cos 2\varphi^{(j)}+8M_0^2\lambda_2 u_{XY}^{(j)}\sin 2\varphi^{(j)}-\mu\Big\}, \tag{3}$$

which is the source of motive force for the setup of the nonzero local parameters.

The local energy density (3) includes the contribution from the magnetic anisotropy (the first term), Zeeman energy (second term), and elastic and magnetoelastic terms. The magnetic energy is represented by the fourth order effective bare in-plane anisotropy constant $\beta_\perp^{(4)}$ and the constant of intraplanar AFM exchange J, and $M_0=|\mathbf{M}_{1,2}|$. Two angles, φ and ψ, describe the orientation of vectors **L** and **H**, correspondingly, with respect to the X axis. The elastic and magnetoelastic properties are described in a standard manner by the shear moduli $c'\equiv(c_{11}-c_{12})/2$ and c_{66} and effective magnetostrictive constants $\lambda_{1,2}$. The tendency for inhomogeneous distribution of the AFM vectors and strains is accounted for by the variables ξ_j, which are volume fractions of the jth-type domain, and the chemical potential μ, which should be equal for all coexisting domains.

Expression (3) includes only the principal terms that influence the DS formation. Thus, we disregard all the local symmetry-conserving interactions (like volume magnetostriction), entropy contribution originating from excitations, which ensures the temperature dependence of the magnetic constants, etc. We also assume that a value of the external field is small enough compared with the characteristic exchange field: $H\ll 2M_0J$, which enables us to exclude from the expressions the small FM vector $M=-(H/J)\sin(\varphi-\psi)\ll L$ (the detailed procedure is described elsewhere; see, for example, Ref. 12). Demagnetization effects are immaterial for the chosen geometry of the sample, and in the general case their contribution $\sim H/2M_0J$ is also negligible.

The ability of the DS to rearrange under the action of the magnetic field crucially depends upon the mobility of the domain walls. We assume that the sample contains a certain amount of the immobile domain walls fixed at the defects, which do not participate in the shift processes under the action of **H**. To distinguish between the different types of the domains we use indices $j=1,2$ for the ''mobile'' and $j=3,4$ for the ''immobile'' ones. The further distinction is related with the orientation of vector **L** in zero magnetic field: $j=1,3$ indicate the domains with $\varphi=0$, and $j=2,4$ those with $\varphi=\pi/2$. Prior to field application, the domains of both types are supposed to be equally represented with probability: $\xi_3(0)=\xi_4(0)=1/2-\xi$.

The parameters of the magnetic structure are obtained from minimization of the free energy $F=F_{stray}+F_{loc}$ [see Eqs. (2) and (3)] with respect to all the variables including the fractions ξ_1 and ξ_2 of the mobile domains.

IV. RECONSTRUCTION OF THE DOMAIN STRUCTURE

Application of **H** results in both rotation of the AFM vectors and shift of the mobile domain walls. The latter takes place below the critical, or monodomenization, field,

$$H_{MD}(\psi)=\frac{H_{1ME}\sqrt{(H_{SF}^2+H_{2ME}^2)\xi}}{\sqrt[4]{(H_{SF}^2+H_{2ME}^2)^2\cos^2 2\psi+H_{1ME}^4\xi^2\sin^2 2\psi}}, \tag{4}$$

at which the domains of one type (say, $j=1$) disappear ($\xi_1=0$). In Eq. (4) the characteristic magnetoelastic

$$H_{1ME}=8M_0^2\lambda_1\sqrt{\alpha' J/c'(\alpha'+c')},$$

$$H_{2ME}=8M_0^2\lambda_2\sqrt{\alpha_{66}J/c_{66}(\alpha_{66}+c_{66})},$$

and pure magnetic (without magnetostriction) spin-flop $H_{SF}=4M_0\sqrt{\beta_\perp^{(4)}J}$ fields are introduced. So, at $H<H_{MD}(\psi)$ redistribution of the DS inside the sample takes place in such a way that the internal (effective) magnetic field is directed along [110] and thus, AFM vectors in the domains are oriented symmetrically with respect to this direction at the angle

$$\varphi_{1,3}=\pi/2-\varphi_{2,4}=-\frac{1}{2}\arcsin\frac{2H_XH_Y}{H_{SF}^2+H_{2ME}^2}. \tag{5}$$

Volume fraction of the domains with the mobile walls depends on **H** as follows:

$$\xi_{1,2}(\mathbf{H})=\xi\mp\frac{(H_{SF}^2+H_{2ME}^2)(H_X^2-H_Y^2)}{2H_{1ME}^2\sqrt{(H_{SF}^2+H_{2ME}^2)^2-4H_X^2H_Y^2}}. \tag{6}$$

In zero field the domains of both types are equally represented, $\xi_1(0)=\xi_2(0)=\xi$.

To elucidate the behavior of the DS at $H>H_{MD}(\psi)$ for a given field direction, let us consider two limiting cases.

The field is directed along the in-plane easy axis for AFM vector ($\psi=0$, i.e., spin-flop case for the domains of the first type) and so, the field does not disturb the equilibrium orientation of **L** vector up to the critical value [see Eq. (4)] $H_{1cr}=H_{MD}(0)=\sqrt{\xi}H_{1ME}$. The shift of the domain walls keeps up a zero internal magnetic field thus excluding rotation of the AFM vectors. The magnitude of the critical field at which the shift processes are accomplished depends upon the number of the mobile domains and is independent of the magnetic anisotropy of the crystal (because the rotation of the magnetic vectors is not involved). Further increase of the field does not influence the magnetic structure at all, until the second critical field, $H_{2cr}=\sqrt{H_{SF}^2+H_{MD}^2(0)}$, is attained. At $H=H_{2cr}$ the internal magnetic field reaches the ''spin-flop'' magnitude at which the vector **L** in unfavorable (with $\mathbf{L}||\mathbf{H}$) immobile domain flops perpendicular to **H**. At $H\geqslant H_{2cr}$ the sample is monodomain, $\xi_1=\xi_3=0,\xi_2=2\xi,\xi_4=1-2\xi$.

The field is applied in hard direction ($\mathbf{H}||[110]$, $\psi=\pi/4$). This configuration is consistent with the symmetrical rotation of the AFM vectors [see Eq. (5)] without a shift of the domain walls, because all types of domains are equivalent. At $H=H_{MD}(\pi/4)=\sqrt{H_{SF}^2+H_{2ME}^2}$ the sample becomes monodomain, with **L** directed perpendicular to **H**, just along the hard direction. The effective field at this point (renormalized by the ''stray'' field, see Ref. 12) is equal to H_{SF}. The field $H_{MD}(\pi/4)$ does not depend upon the mobility of the domains, but includes the value of magnetic anisotropy, which governs the rotation of spins. Further increase of the **H** field does not affect the orientation of **L** vectors.

In the case of arbitrary directed **H**, reorientation of the AFM vector **L** is always incomplete; the value of the second critical field is not defined, but the field of monodomenization should be noticeably greater than H_{SF}. When **H** is removed, the behavior of the DS strongly depends upon the mobility of the domain walls and relaxation time of the strains as well. If this time is smaller than the rate of **H** sweeping, the strain field in the sample can be treated as unfrozen and the behavior of the DS should be reversible, as it, e.g., takes place in a magnetostriction experiments.[16] Slight irreversibility can arise from the necessity for vector **L** to overcome the hard direction when flopping back from *Y* to *X* direction (if **H** is close to *X*). In the opposite case, when the relaxation time is greater than **H** sweeping rate, the strains are partially frozen. The corresponding effective field in the sample is renormalized as follows:

$$H_{eff}=\{[H_X^2-H_Y^2+16M_0^2J\lambda_1(u_{XX}^{froz}-u_{YY}^{froz})]^2 +4[H_XH_Y+16M_0^2J\lambda_2u_{XY}^{froz}]^2\}^{1/4}, \tag{7}$$

where $\hat{u}^{froz}$ is the ''frozen'' (unrelaxed) part of magnetostriction. This gives rise to the shift of the monodomenization field toward a lower absolute value and should reveal itself in the hysteresis phenomena.

V. RESULTS

At $H\leqslant H_{1cr}$ the field dependence of MR can be obtained after substituting Eqs. (5) and (6) into Eq. (1) and averaging over the sample:

$$\rho_{XX}(\mathbf{H})-\rho_{is}=-\aleph_1\frac{H_X^2-H_Y^2}{H_{1ME}^2}-\aleph_2\left(\frac{H_XH_Y}{H_{MD}^2(\pi/4)}\right)^2,$$

$$\rho_{YY}(\mathbf{H})-\rho_{is}=\aleph_1\frac{H_X^2-H_Y^2}{H_{1ME}^2}-\aleph_2\left(\frac{H_XH_Y}{H_{MD}^2(\pi/4)}\right)^2, \tag{8}$$

$$\rho_{ZZ}(\mathbf{H})-\rho_{ZZ}(0)=-\frac{M_0^2\eta_{31}^L}{2J^2}\left[H^2+\frac{(H_X^2-H_Y^2)^2}{H_{1ME}^2}+\frac{4H_X^2H_Y^2}{H_{MD}^2(\pi/4)}\right]-\eta_{312}^L\left(\frac{4M_0^2H_XH_Y}{H_{MD}^2(\pi/4)}\right)^2,$$

$$\rho_{XY}(\mathbf{H})=-\frac{4M_0^2\eta_{66}^LH_XH_Y}{H_{MD}^2(\pi/4)},$$

$$H_{MD}^2(\pi/4)=H_{SF}^2+H_{2ME}^2. \tag{9}$$

In expressions (8) we have set up the isotropic field independent part of the in-plane resistivity:

$$\rho_{is}=\rho_{aa}^{(0)}+2M_0^2(\eta_{11}^L+\eta_{12}^L)+8M_0^4(\eta_{111}^L+\eta_{122}^L), \tag{10}$$

and that of the out-of-plane resisitivity:

$$\rho_{ZZ}(0)=\rho_{cc}^{(0)}+4M_0^2\eta_{31}^L. \tag{11}$$

The combinations

$$\aleph_1=2M_0^2[\eta_{11}^L-\eta_{12}^L+4M_0^2(\eta_{111}^L-\eta_{122}^L)],$$

$$\aleph_2=16M_0^4[\eta_{111}^L-\eta_{112}^L+\eta_{122}^L],$$

are the phenomenologic coefficients of correspondingly anisotropic and isotropic MR, induced by the AFM ordering.

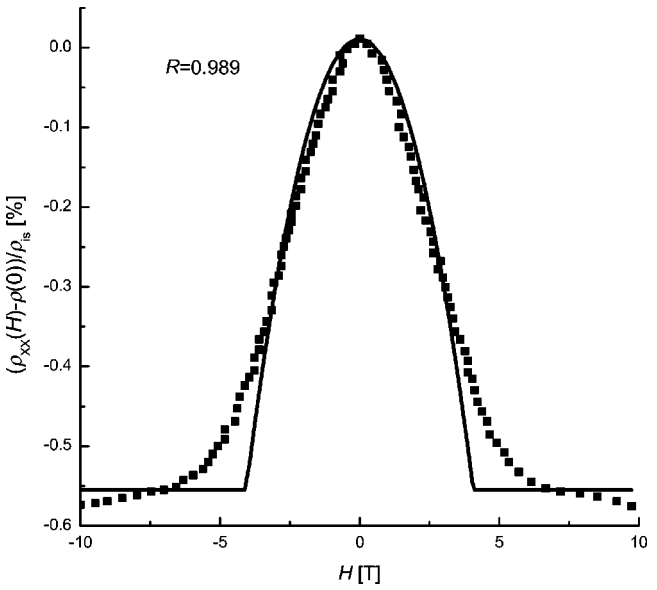

FIG. 1. Low-field dependence of longitudinal in-plane AMR of $YBa_2Cu_3O_{6.3}$ at 30.1 K, $\mathbf{H}||\mathbf{a}$. Solid line, theoretical curve $[\rho_{XX}(\mathbf{H})-\rho_{XX}(0)]/\rho_{is}$; squares, experiment (Ref. 2).

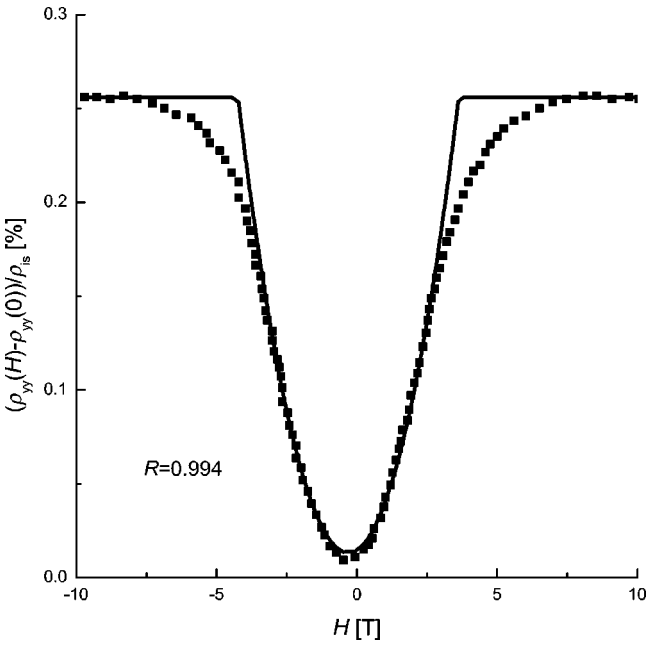

FIG. 2. Low-field dependence of the transverse in-plane AMR of $YBa_2Cu_3O_{6.3}$ at 20 K, $\mathbf{H}||\mathbf{a}$. Solid line, theoretical curve $[\rho_{YY}(\mathbf{H})-\rho_{YY}(0)]/\rho_{is}$; squares, experiment (Ref. 2).

It follows from Eq. (8) that the main contribution of the magnetic field that is quadratic in H gives rise to an anisotropy of the in-plane resistivity, i.e., the field induces the nonzero values $\rho_{XX}-\rho_{YY},\rho_{XY}$. The out-of-plane component of MR, $\rho_{ZZ}(\mathbf{H})$, is weakened due to the exchange constant J, and dependence upon the field direction arises only in the fourth order term.

At large $H \gg H_{MD}$ the sample is monodomain, the vector $\mathbf{L}$ is oriented almost perpendicularly to $\mathbf{H}$, so

$$\rho_{XX}(\mathbf{H})-\rho_{is}=-\aleph_1\cos 2\psi-\aleph_2\cos^2 4\psi - M_0^2H^2(\eta_{11}^L+\eta_{12}^L)/2J,$$

$$\rho_{YY}(\mathbf{H})-\rho_{is}=\aleph_1\cos 2\psi-\aleph_2\cos^2 4\psi - M_0^2H^2(\eta_{11}^L+\eta_{12}^L)/2J,$$

$$\rho_{ZZ}(\mathbf{H})-\rho_{ZZ}(0)=-\frac{M_0^2H^2\eta_{31}^L}{J^2} - \frac{4M_0^4\eta_{312}^L H_{MD}^4(\psi)\sin^2 2\psi}{\xi^2(H_{2ME}^2+H_{SF}^2)^2}. \quad (12)$$

An angular dependence of MR arises mainly from the orientation of the external field, and the direction-independent background proportional to $\sim H^2$ arises from the nonzero magnetization $M=H/2M_0J$.

VI. COMPARISON WITH EXPERIMENT

For the numerical comparison with the theory developed we used the data obtained in Ref. 2. All the measurements have been performed with a $YBa_2Cu_3O_{6.3}$ single crystal and the authors present the field dependence of the relative value of MR, i.e., $[\hat{\rho}(\mathbf{H})-\hat{\rho}(0)]/\rho(0)$. Figure 1 shows the low-field dependence of longitudinal MR of measured at $T=30.1$ K, $\mathbf{H}||X$, along with approximation of $[\rho_{XX}(\mathbf{H})-\rho_{XX}(0)]/\rho_{is}$ calculated from Eqs. (8) and (12) with $H_{1ME}=4.1$ T, $(\aleph_1/\rho_{is})=-0.57$, $\xi=0.5$. In Fig. 2 the analogous dependence of the transverse MR (Ref. 17) measured at $T=20$ K, $\mathbf{H}||X$; theoretical dependence $[\rho_{YY}(\mathbf{H})-\rho_{YY}(0)]/\rho_{is}$ was taken from Eqs. (8) and (12) with $H_{1ME}=4.03$ T, $(\aleph_1/\rho_{is})=-0.26$. Theoretical approximation for these two cases were made with the use of two adjusting parameters. One of them, H_{1ME}, coincides with the monodomenization field $H_{MD}(0)$ for $\mathbf{H}$ directed along an easy axis. The value of H_{1ME} is calculated as a coefficient in $[\hat{\rho}(\mathbf{H})-\hat{\rho}(0)]/\rho(0)$ dependence. It can be also roughly evaluated when considering the magnetoelastic energy (see below). The second parameter, $(\aleph_1/\rho_{is})$, which is a zero-field relative MR of the monodomain sample, was deduced from the extrapolation of the high-field section of the MR curve to $H=0$. Experimental data were taken after a number of field sweepings, so, hysteresis (shift of monodomenization field $\delta H_{hys}=0.3$ T) and residual resistivity (0.013%) are observed. Figure 3 shows the dependence of in-plane AMR on the angle between $\mathbf{H}$ and electric current at 30 K, $\mathbf{H}\perp\mathbf{c}$, $H=16$ T and theoretical curve $[\rho_{XX}(\mathbf{H})-\rho_{is}]/\rho_{is}$ as well, calculated from Eq. (12) with $(\aleph_1/\rho_{is})=-0.48$, $(\aleph_2/\rho_{is})=0.15$. In this case the adjusting parameters $(\aleph_{1,2}/\rho_{is})$ where derived as of the curve $(\rho_{XX}-\rho_{is})/\rho_{is}$ vs $\cos 2\psi$. In all the figures the correlation coefficients R are included.

Figures 1 and 2 clearly show the quadratic field dependence of the AMR, in agreement with the theoretical predictions. At high H the angular dependence of $\rho_{anis}(\psi)$ has a ''d-wave''-like symmetry with opposite sign and slight difference in value between the perpendicular-oriented petals (Fig. 3). This shape is satisfactorily described by formula

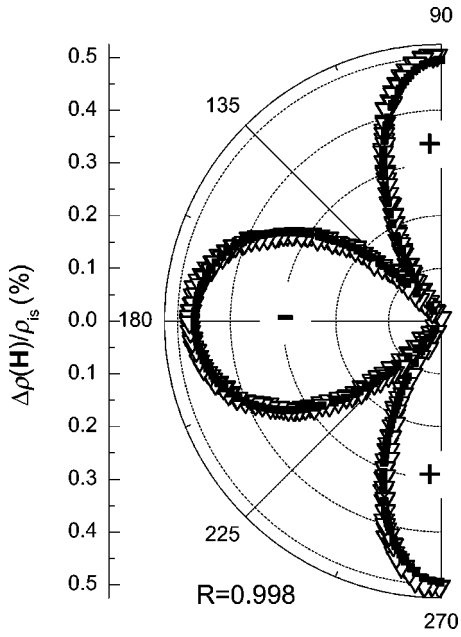

FIG. 3. Dependence of in-plane AMR on the angle between H and electric current at 30 K, $\mathbf{H}\perp\mathbf{c}$, $H=16$ T. Solid line, theoretical curve $[\rho_{anis}(\psi)]/\rho_{is}$; cirles, experiment (Ref. 2). The sign of the MR is indicated.

(12). It should be underlined that the adjusting parameters for the high-field (monodomain) region are close to those calculated for the low-field (polydomain) region, where almost complete reversibility is observed.

VII. DISCUSSION

The developed theory explains the peculiarities of the in-plane MR at different magnetic field and temperature values by the behavior of thermodynamically equilibrium DS under the action of **H**. Quite good qualitative (with Ref. 1) and quantitative (with Ref. 2) agreement with the experiment and experimental evidence of the existence and reversibility of the DS (Refs. 3 and 7) make it possible to consider the mechanism proposed as one of the main ones. It is interesting that because of the magnetoelastic nature of AFM domains, the spontaneous strain value 0.3% can be easily evaluated from the typical value of monodomenization field and shear modulus: $H_{MD}\propto H_{ME}\propto 4$ T and $c'\propto\alpha'\propto 130$ GPa. The domain-related features of the behavior of the AFM in question make it possible to compare it with the well-known thermoelastic alloys (e.g., InTl, Cu-Al-Zn, TiNi, etc.). As thermoelastic martensites, the AFM shows the shape memory effect (below 30 K the hysteresis becomes more and more pronounced and the crystal reproduces the same field dependence after a number of field sweepings). This opens the way to manipulate the DS and thus, resistivity, by applying the stress. The experimental investigation of the sample magnetostriction in the external magnetic field and stress dependence of MR can confirm or withdraw the hypothesis of the magnetoelastic domains. Really, the same results as given by Eqs. (8)–(12) could be obtained if one substitutes H^2 for

$$16M_0^2 J\sqrt{(\lambda_1/c')^2(\sigma_{XX}-\sigma_{YY})^2+(\lambda_2/c_{66})^2\sigma_{XY}^2}$$

and ψ for

$$(1/2)\arctan\frac{\lambda_2 c'\sigma_{XY}}{\lambda_1 c_{66}(\sigma_{XX}-\sigma_{YY})},$$

where $\hat{\sigma}$ is a stress tensor. In the simplest case with $\sigma_{XY}=0$, the stress of monodomenization, $(\sigma_{XX}-\sigma_{YY})_{MD}=4M_0^2\lambda_1\alpha'\xi/(\alpha'+c')$, should be $\propto 100$ MPa, as estimated from the above-mentioned data. DS should also result in the peculiarities of AFMR spectra, namely, monodomenization of the sample gives rise to freezing of the spontaneous strains and hardening of low-frequency gap in the AFMR spectra (for the details of the effects see Refs. 12 and 16).

ACKNOWLEDGMENTS

The authors would like to thank Dr. E.B. Amitin for the valuable discussions and help in the analysis of experimental data, Professor M.A. Ivanov, Professor V.I. Marchenko, and Professor S.M. Ryabchenko for discussions and critical comments. E.V.G. is grateful to A.A. Malyshenko for the financial and technical support. The research of V.M.L was partly supported by Swiss National Science Foundation (SCOPES Project No. 7UKPJ062150.00/1).

[1] E.B. Amitin *et al.*, Pis'ma Zh. Eksp. Teor. Fiz. **70**, 350 (1999) [JETP Lett. **70**, 312 (1999)].

[2] Y. Ando, A.N. Lavrov, and K. Segawa, cond-mat/0004135 (unpublished).

[3] A. Janossy, F. Simon, and T. Fehèr, cond-mat/0005275 (unpublished).

[4] A.N. Lavrov, M.Yu. Kameneva, and L.P. Kozeeva, Phys. Rev. Lett. **81**, 5636 (1998).

[5] Y. Ando, A.N. Lavrov, and K. Segawa, Phys. Rev. Lett. **83**, 2813 (1999).

[6] P. Burlet, J.Y. Henry, and L.P. Regnault, Physica C **296**, 205 (1998).

[7] A. Janossy, F. Simon, T. Fehèr, A. Rockenbauer, L. Korecz, C. Chen, A.J.S. Chowdhury, and J.W. Hodby, Phys. Rev. B **59**, 1176 (1999).

[8] Another mechanism based on the effective hole transport through low lying oxygen state was recently proposed in Ref. 9.

[9] A.S. Moskvin and Yu.D. Panov, cond-mat/0008035 (unpublished).

[10] For the description of the dynamical properties of $RBa_2Cu_3O_x$ the rigorous (and more complicated) four-sublattice model should be used (Ref. 11).

[11] V.G. Baryakhtar, V.M. Loktev, and D.A. Yablonskii, Physica C **156**, 667 (1988).

[12] E.V. Gomonaj and V.M. Loktev, Fiz. Niz. Temp **25**, 699 (1999) [Low Temp. Phys. **25**, 520 (1999)]; Acta Phys. Pol. A **97**, 459 (2000).

[13] E.V. Gomonaj and V.M. Loktev, cond-mat/0010258, J. Phys.: Condens. Matter (to be published).

[14] Usually, the main contribution to the surface tension is linear in the shear components of strain tensor (Ref. 15), but for [001]-oriented films nontrivial terms are quadratic [as in Eq. (2)].

[15] V.I. Marchenko and A.Ya. Parshin, Zh. Éksp. Teor. Fiz. **79**, 257 (1980) [Sov. Phys. JETP **52**, 129 (1980)].

[16] V.M. Kalita, A.F. Losenko, S.M. Ryabchenko, and P.A. Trotsenko, Ukr. Fiz. Zh. **43**, 1469 (1998).

[17] The authors of Ref. 2 have subtracted high-field quadratic background [see Eq. (12) for isotropic field-dependent contribution], which gives rise to a lower value of $(\aleph_1/\rho_{is})$ compared with Fig. 1.